INGENIERÍA QUÍMICA

Descripción teórica y experimental del equilibrio de adsorción de soluciones iónicas en la superficie de los sistemas γ-Al_2O_3 y MoO_3/γ-Al_2O_3

Fiderman Machuca-Martínez[*], José L. G. Fierro[§]**

**Laboratorio de Investigación en Catálisis y Procesos. Escuela de Ingeniería Química, Universidad del Valle, A.A. 25360. Cali, Colombia.*

***Instituto de Catálisis y Petroleoquímica, CSIC, Cantoblanco, 28049 Madrid, España.*

§ e-mail: jlgfierro@icp.csic.es

(Recibido: Enero 13 de 2010- Aceptado: Abril 3 de 2010)

Resumen

Se estudiaron las isotermas de adsorción en equilibrio de iones Mo, Co y Pt sobre γ-Al_2O_3 y iones Co y Pt sobre MoO_3/γ-Al_2O_3. Los catalizadores molibdeno alúmina para los ensayos de adsorción fueron preparados por impregnación de los soportes de alúmina con heptamolibdato de amonio. Los datos de equilibrio de adsorción fueron obtenidos a partir del proceso de adsorción liquido-sólido. Las curvas de adsorción fueron tipo L para los sistemas Mo y Co sobre γ-Al_2O_3 y Co(Pt) sobre MoO_3/γ-Al_2O_3, mientras para el sistema Pt(Co) sobre MoO_3/γ-Al_2O_3 fueron tipo S. Para el caso del molibdeno, se encontró que las especies en solución (tetraédricas y octaédricas) afectan la adsorción del molibdeno. La adsorción de iones Co(II) sobre alúmina o alúmina modificada no depende de la alúmina utilizada. La forma de las isotermas de adsorción de iones Co sobre MoO_3/γ-Al_2O_3 parece ser modificada cuando los iones Pt(IV) están presentes simultáneamente. Los procesos de adsorción de especies de Pt dependen de la presencia de Mo(VI) y Co(II) en la superficie de los soportes. Se observó que la cantidad de Pt adsorbido sobre MoO_3/γ-Al_2O_3 disminuye en presencia de iones Co(II) en solución. Finalmente, se calcularon los parámetros de adsorción en equilibrio de los sistemas Mo(VI) and Co(II) sobre γ-Al_2O_3 and Co(II) y/o Pt(IV) sobre MoO_3/γ-Al_2O_3.

Palabras Claves: Adsorción en equilibrio, Adsorción líquido sólido, Isotermas de adsorción, Alúmina, Molibdeno, Platino, Cobalto, Preparación de catalizadores.

CHEMICAL ENGINEERING

Experimental and theoretical description of the equilibrium adsorption of metal ion solutions on the surface of γ-Al_2O_3 and MoO_3/γ-Al_2O_3 systems

Abstract

The equilibrium adsorption isotherms of Mo, Co and Pt species on γ-Al_2O_3 and Co and Pt on MoO_3/-Al_2O_3 oxides were studied. The Molybdena-alumina catalysts for adsorption tests were prepared by impregnation of γ-Al_2O_3 supports with aqueous solutions of ammonium heptamolybdate. The equilibrium adsorption data were obtained from liquid-solid adsorption process. L-type shaped adsorption curves were found for Mo and Co on γ-Al_2O_3 and Co(Pt) on MoO_3/γ-Al_2O_3 whereas S-shaped were found in the Pt(Co) on MoO_3/γ-Al_2O_3 systems. In the Mo system, it was found that the molybdenum species in solution (tetrahedral and octahedral) affected the Mo adsorption. The adsorption of Co(II) ions over alumina or modified alumina did not depend on the alumina source. The shape of the Co adsorption isotherm on MoO_3/γ-Al_2O_3 appeared to be modified when Pt(IV) ions were present simultaneously. The adsorption process for Pt species depended on the presence of Mo(VI) and Co(II) ions on the supports surface. It was observed that the amount of Pt adsorbed on the surface of the MoO_3/γ-Al_2O_3 sample decreased in the presence of Co(II) ions in solution. Finally, the equilibrium parameters for the adsorption of Mo(VI) and Co(II) on γ-Al_2O_3 and Co(II) and/or Pt(IV) on MoO_3/γ-Al_2O_3 were determined.

Keywords: Equilibrium adsorption, Liquid solid adsorption, Adsorption isotherms, Alumina, Molybdenum, Platinum, Cobalt, Catalysts preparation.

1. Introducción

The need for better hydrotreating catalysts has promoted the research into new catalytic systems. The new generation noble metal-promoted MoO_3/Al_2O_3 systems, noble metal/Al_2O_3 and different combinations of these can exhibit different performances not only in hydrotreatment reactions of oil fractions but also in other reactions, i.e. isomerization and hydrogenation processes, NOx abatement, partial oxidation and olefin metathesis, Kubota *et al*. (2010), Achchar *et al*. (2009), Baldovino-Medrano *et al*. (2009), Chianelli *et al*. (2009), Roukoss *et al*. (2009), Eliche-Quesada *et al*. (2007), Lamonier *et al*. (2007), Klimova *et al*. (2009), Kurhinen & Pakkanen (2000), Navarro *et al*. (2000), Schmal *et al*. (1999), Klimova *et al*. (1998), Regalbuto *et al*. (1999), Griboval *et al*. (1998).

Studies on the adsorption of metal ions on the surface of metal oxides are important in many fields, such as soil chemistry, geochemistry, colloid science and catalytic chemistry. In latter case, fundamental knowledge of the impregnation steps is crucial for the development of the new generation of catalysts, Kubicka & Kaluza (2010), Pashigreva *et al*. (2009), Semagina & Kiwi-Minsker (2010), Bourikas *et al*. (2006), Chianelli *et al*. (2009), Komiyama (1985), Vissenberg *et al*. (2000), van Veen *et al*. (1990), Lutra & Cheng (1987), Wang & Hall (1982), Hachiya *et al*. (1984), Gajardo *et al*. (1980), Giordano *et al*. (1975). Thus, in recent decades several adsorption models have been proposed to explain the equilibrium of adsorption of several metal cations and anions from liquid solutions. Most equations, that express the adsorption isotherms in an analytical way, have been worked out for gases, i.e. Langmuir, Freundlich and BET isotherms; however, adsorption from solutions is much more complex. This complexity is reflected in the shape of the adsorption curve, Pashigreva et al. (2009), Roukoss et al. (2009), Bourikas et al. (1998, 1996, 2006), Baumgarten & Kirchhausen-Dusing (1997), Pizzio et al. (1996), van Veen et al. (1987), Siri et al. (1985), Tewari et al. (1975). Study of the genesis of the equilibrium isotherms should lead to deeper insight into the nature of the processes responsible for the initial catalyst structure. All this information can be used to understand and to model catalytic phenomena.

Within this context, the present work was undertaken to determine the equilibrium parameters of Mo(VI) and Co (II) ion adsorption on alumina with different precursors and, simultaneously, to explore their effects in the adsorption process. As a further goal, the adsorption of Co(II) and Pt(IV) ions onto molybdenum oxide-loaded alumina was attempted.

2. Experimental Procedure

2.1 Catalyst Preparation

Three γ-Al_2O_3 supports from Akzo (BET area of 189 m^2/g; mean pore diameter determined by the BJH method of 7.64 nm, and pore volume of 0.51 cm^3/g), Rhone-Poulenc (BET area of 196 m^2/g; mean pore diameter of 8.84 nm, and pore volume of 0.50 cm^3/g), and Procatalyse (BET area of 228 m^2/g; mean pore diameter of 8.87 nm and pore volume of 0.50 cm^3/g) were used.

Molybdena-alumina catalysts used like supports for adsorption tests were prepared by impregnation of γ-Al_2O_3 supports with aqueous solutions of ammonium heptamolybdate (AHM, Merck), whose concentration was selected in order to obtain surface concentrations close to the theoretical monolayer of MoO_3 on the γ-alumina. The preparation conditions have been reported in a previous work, Machuca et al. (2001). Here, the samples are labeled as MoO_3/γ-Al_2O_3 (AK), MoO_3/γ-Al_2O_3 (RO) and MoO_3/γ-Al_2O_3 (PR), where AK, RO and PR refer to the Akzo, Rhodia and Procatalyse supports, respectively.

2.2 Determination of Equilibrium Adsorption Isotherms

The equilibrium adsorption data were obtained from the liquid solid adsorption processes. The isotherms were obtained following a typical procedure, reported previously, Machuca et al. (2001). Aqueous molybdenum, cobalt and platinum solutions were prepared from ammonium heptamolybdate (AHM, Merck), sodium molybdate dihydrate (SoMo, Merck), cobalt (II), nitrate hexahydrate (CoNi, Sigma), cobalt (II) chloride hexahydrate (CoCl, Aldrich),

cobalt (II) acetate tetrahydrate (CoAc, Aldrich) and hexachloroplatinic acid (Sigma); deionized water (Milli Q quality, 18.2 μΩ) was used in all cases.

2.3 Catalyst Characterization

The metal content of the calcined samples was determined using a Perkin Elmer Optima 3300 DV inductively coupled plasma optical emission spectrometer (ICP-OES). The texture (area, mean pore diameter and pore volume) of the supports and calcined catalysts was determined from the nitrogen adsorption isotherms using a Micromeritics Digisorb 2600 automatic apparatus. DRS and UV-Vis spectra of the catalyst samples and the precursors (solid and aqueous solutions) were collected on a Shimadzu UV-2100 spectrophotometer, in the 190900 nm range, using $BaSO_4$, alumina or water as references, respectively.

3. Results and Discussion

It is generally accepted that two kinds of coordination structures of surface molybdate species (tetrahedral and octahedral) exist on the γ-Al_2O_3 surface. Tetrahedral molybdenum oxide species are related to the isolated species, whereas octahedral molybdate species are polymerized structures. Despite this current consensus, the genesis and development of molybdate surface during preparation steps is still controversial, even though they have been studied in depth, Bejenaru *et al*. (2009), Baldovino-Medrano *et al*. (2009), De Lacaillerie & Gan (2007), Frizi *et al*. (2008), Bergwerff *et al*. (2008), Chianelli *et al*. (2009), Klimova *et al*. (2009), Lutra & Chebg (1987), Mestl & Srinivasan (1998), de Wilmar *et al*. (1998). From all the works carried out to date, several scenarios emerge. Firstly, Jeziorowski and Knözinger, Mestl & Srinivasan (1998), proposed that MoO_4^{-2} ions are developed on the alumina surface irrespective of the impregnating solution pH, although these species become polymerized during the calcination step, thus leading to octahedral structures. The second model was advanced by Wang and Hall; Wang & Hall (1982), Mestl & Srinivasan (1998), who pointed out that the adsorbed molybdate species depend on the impregnation solution pH: at high pH, only tetrahedral molybdate ions are adsorbed onto the γ-Al_2O_3 surface, whereas at low pH the adsorption of polymolybdate ions (octahedral symmetry) dominates. Then, Xiong et al. (2000) reported that the coordination structures of the surface species are essentially influenced by the net pH value at the surface region of the support. Rencently, Bergwerff et al. (2008), reported that there are interactions between Co Mo ions in solutions and that this can have consequences for the preparation of supported CoMo HDS catalysts. In this case, the CoMo-complexes can be formed on the catalyst surface, where the Co(II) is bound to the outside the molybdate-ions.

3.1 pH and adsorption behavior

3.1.1 Mo/γ-Al_2O_3 systems

Spectroscopic studies (UV-Vis) were performed to determine the ionic species present in solution; in parallel, the DRS UV-Vis spectra of the impregnated solids were recorded. Although the use of aqueous molybdate solutions is debatable, Bergwerff *et al*. (2008), Duan et al. (2007), Weber (1995), Fournier *et al*. (1989), due to the complex chemistry of molybdate ions in solution, the approach undertaken here is reasonable.

Although the tetrahedral MoO_4^{2-} ion can be protonated in solution and its coordination sphere is solvated by H_2O, leading to an increase in the Mo coordination number, Fournier *et al*. (1989), this process will lead to an overlapping in the absorption UV-Vis region with the octahedral molybdenum species. Along the preparation of MoO_3/alumina samples, carried out by impregnation of alumina with aqueous solutions of Na_2MoO_4, Xiong *et al*. (2000) found that in the wet, dry and calcined states all the samples exhibited Mo species that were tetrahedrally coordinated by oxygen ions, even after calcination. In the present work, the UV-Vis spectra of Mo, Co and Pt solutions were used to identify the nature of molybdenum oxo-species in solution. On the other hand, the comparison of the DR spectra of the salt precursors and the impregnated samples, allows one to distinguish among the molybdenum species present on the support surface. Apart from this, other techniques

have been used to unveil the symmetry and nature of the adsorbed species (i.e. optical band-gap energy, Eg and Gaussian analysis) from DRS/UV-Vis spectra, Weber (1995), Fournier *et al*. (1989).

Along the adsorption of metal ions on the alumina surface, the pH values of the impregnating solution were seen to change. Table 1 compiles both the initial and final pH ranges for all the systems under study. From these data, it is clear that the pH of the solution changes not only along the impregnation process but also with the initial concentration of the impregnating solution. Although the type of anionic species present in molybdate solutions depends on their pH value, Bergwerff *et al*. (2008), Regalbuto *et al*. (1999), Lutra & Cheng (1987), Mestl & Srinivasan 1998), under the nearly acid solutions employed in the present work most of the molybdenum species in solution were polymeric ions (octahedral symmetry) because the ionic equilibrium was shift to the left-hand side:

$$Mo_7O_{24}^{6-} + 4\ H_2O \Leftrightarrow 7\ MoO_4^{2-} + 8\ H+ \qquad (1)$$

Therefore, the adsorption of molybdate ions $(Mo_7O_{24})^{6-}$ shifts the pH to values close to point of zero charge of the support at the end of impregnation. Figure 1 shows the pH change at adsorption equilibrium. In all cases, the final pH values are higher than the initial ones. This type of behavior is similar to that observed by Spanos et al. (2006, 1990) for a similar system. However, the comparison of the final pH values for the adsorption of molybdate ions on alumina revealed some differences, although they were considered no significant.

Contrariwise, most solution oxo-molybdenum species present during the impregnation with SoMo salt were monomeric (MoO_4^{-2}) species in tetrahedral symmetry. In this case, the change in pH values became smaller than those originated upon AHM impregnation (see Table 1). This observation can be related to the extent of adsorption, which in turn was substantially lower than that observed for AHM solutions. This can be explained as being due to a weak interaction between the monomeric ions and the adsorption sites. These results are in agreement with the reported by several authors, Iannibello & Mitchell (1979), Weigold (1983), Butz *et al*. (1989), Plyuto *et al*. (1997) and Jiang *et al*. (2008).

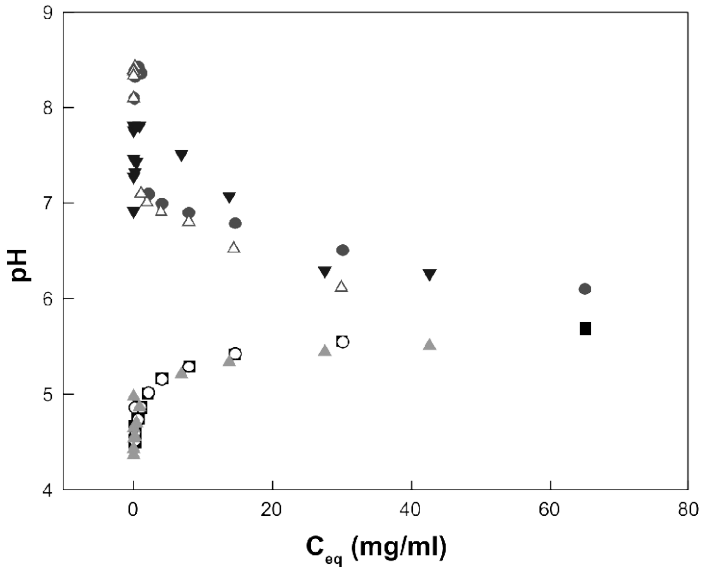

Figure 1. pH vs. Ceq profiles. Adsorption of AHM solution over alumina: (■) final pH γ-Al_2O_3 (AK), (•) initial pH γ-Al_2O_3 (AK); (○) initial pH γ-Al_2O_3 (RO), (Δ) final pH γ-Al_2O_3 (RO) ; (▲) initial pH γ-Al_2O_3 (PR), (▼) final pH γ-Al_2O_3 (PR).

Table 1. pH values for metal ion adsorption on γ-Al_2O_3 or MoO_3/γ-Al_2O_3

System[a]	Alumina	Initial Range pH	Final Range pH	pH_{ZPC} Support	Initial content. range (mg /mL)[b]
AHM/γ-Al_2O_3	AK	4.87 – 5.70	6.40 – 7.72	7.56	0.013 – 65.00
AHM/γ-Al_2O_3	RO	4.87 – 5.70	6.11 – 8.10	7.84	0.013 – 65.00
AHM/γ-Al_2O_3	PR	4.49 – 4.96	6.26 – 7.28	7.72	0.013 – 42.50
SoMo/γ-Al_2O_3	AK	7.14 – 7.32	7.36 – 8.72	7.56	0.013 – 29.98
SoMo/γ-Al_2O_3	RO	7.14 – 7.32	8.42 – 8.24	7.84	0.013 – 29.98
SoMo/γ-Al_2O_3	PR	7.06 – 7.14	7.50 – 8.62	7.72	0.055 – 26.00
CoNi/γ-Al_2O_3	AK	7.04 – 6.57	6.96 – 5-.65	7.56	0.005 – 6.200
CoNi/γ-Al_2O_3	RO	7.04 – 6.57	7.60 – 4.77	7.84	0.005 – 6.200
CoNi/γ-Al_2O_3	PR	6.37 – 5.08	7.61 – 5.54	7.72	0.021 – 11.07
CoCl/γ-Al_2O_3	AK	7.50 – 4.55	5.66 – 5.79	7.56	0.006 – 6.200
CoCl/γ-Al_2O_3	RO	7.50 – 4.55	7.54 – 5.90	7.84	0.006 – 6.200
CoCl/γ-Al_2O_3	PR	7.02 – 7.50	6.05 – 5.55	7.72	0.0016 – 5.80
CoAc/γ-Al_2O_3	AK	8.08 – 7.27	7.04 – 5.80	7.56	0.008 – 6.300
CoAc/γ-Al_2O_3	RO	8.08 – 7.27	7.38 – 5.69	7.84	0.008 – 6.300
CoAc/γ-Al_2O_3	PR	7.02 – 7.50	7.15 – 5.73	7.72	0.0016 – 5.80
Co/MoO_3-γ-Al_2O_3	AK	6.71 – 6.57	3.30 – 3.68	3.62	0.750 – 13.00
Co/MoO_3-γ-Al_2O_3	RO	6.71 – 6.57	3.87 – 3.80	3.80	0.750 – 13.00
Pt/MoO_3-γ-Al_2O_3	AK	2.20 – 1.57	3.65 – 3.60	3.62	0.500 – 3.300
Pt/MoO_3-γ-Al_2O_3	RO	2.20 – 1.57	3.73 – 3.82	3.80	0.500 – 3.300
Pt-(Co)/MoO_3-γAl_2O_3	AK	2.67 – 4.04	3.39 – 3.86	3.62	0.030 – 0.120
Co-(Pt)/$MoO_3\gamma Al_2O_3$	AK	2.67 – 4.04	3.39 – 4.86	3.62	0.270 – 8.500

[a]Solution with support; [b]Amount of metal ion in solution; [c]Solution with two ions

Since the alumina sites involved in the impregnation with AHM and SoMo salts was virtually the same, the surface had greater affinity for the polymeric species. This behavior could be related with the species on surface of supports, this species could change with the adsorption conditions, especially the pH. These results are in agreement with the findings of Luthra & Cheng (1987), Hall & Wang (1982) and Al-Dalama *et al*. (2005).

The electronic spectra of AHM and SoMo solutions are shown in Figs. 2 and 3, respectively.

The positions of the absorption bands are also compiled in Table 2. With increasing molybdenum concentrations, the main band shifted toward a higher wavelength. However, SoMo solutions exhibited a shoulder at 234 nm, whose position did not change with increasing Mo concentrations. This shoulder was also observed in AHM solutions, although it shifted slightly with the Mo concentration. For SoMo solutions, the shoulder was overshadowed by an intense band at around 250 nm, and disappeared at Mo concentrations over 250 ppm.

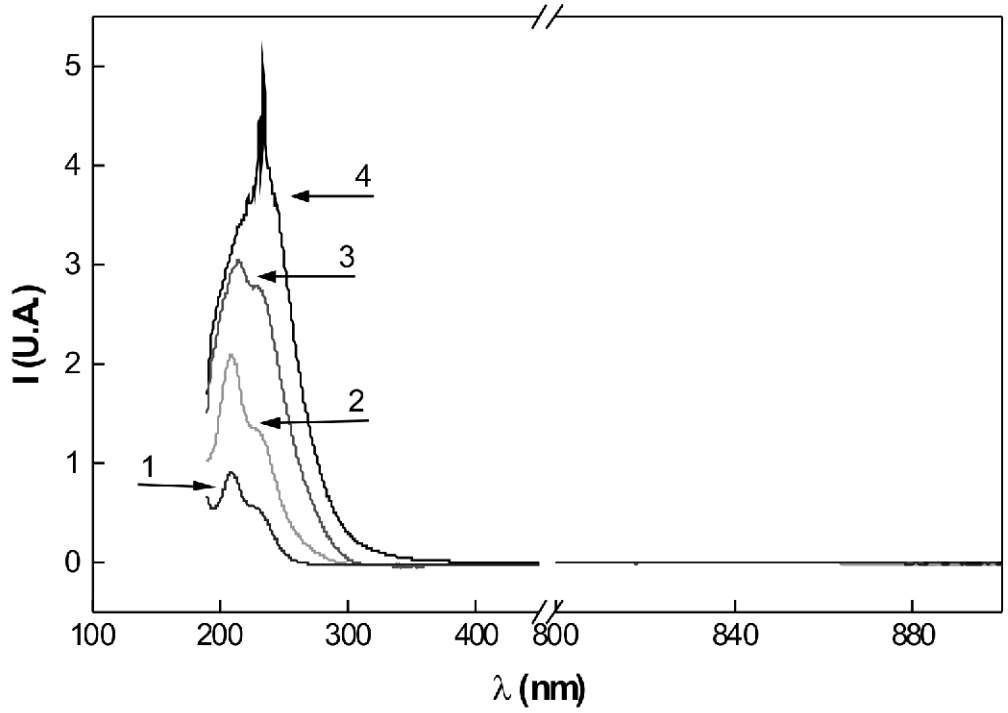

Figure 2. Uv-Vis spectra of AHM solutions. (1) 13 ppm; (2) 30 ppm; (3) 60 ppm; (4) 120 ppm

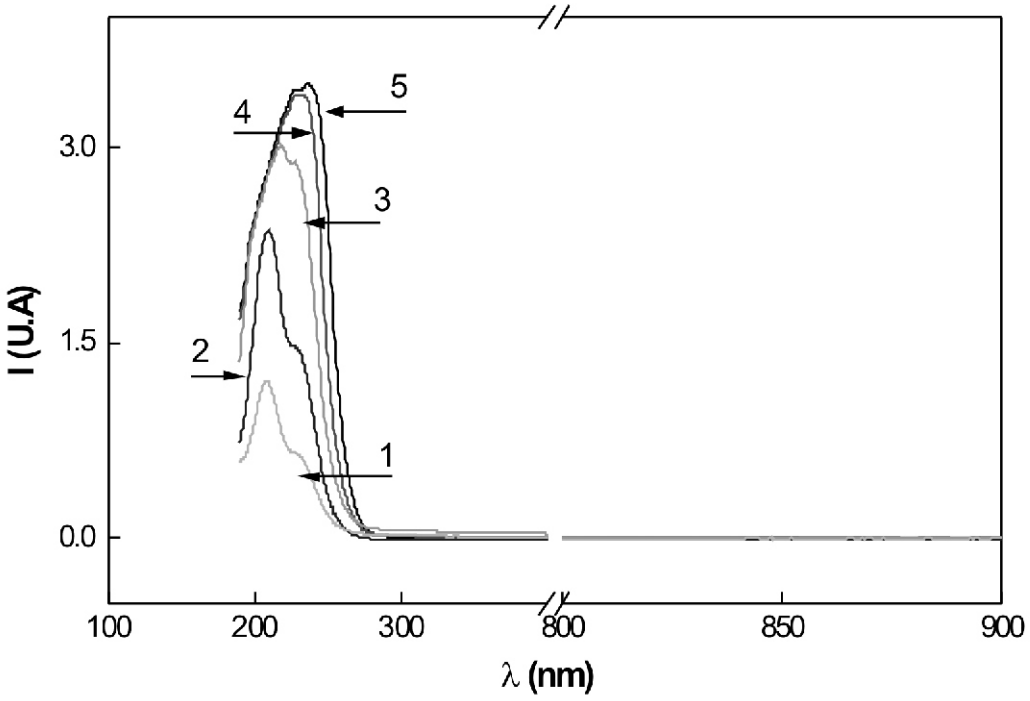

Figure 3. Uv-Vis spectra of SoMo Solutions. (1) 13 ppm ; (2) 33 ppm ; (3) 65 ppm ; (4) 130 ppm ; (5) 250 ppm

Table 2. Principal bands in UV-Vis spectra and pH for AHM and SoMo Solutions

Solution System	Dominant molybdate species	Initial pH	Mo Concentration (ppm)	Mean Band Peak (nm)	Shoulder (nm)
AHM	Polymeric	4.51	120	231.0-234.5[a]	
		4.53	60	214.0	235.5
		4.67	30	209.5	234.5
		4.87	13	209.0	234.0
SoMo	Monomeric	7.17	250	237.0[b]	
		7.31	130	233.0[b]	
		7.10	65	218.0	234.0
		7.24	33	209.5	234.0
		7.14	13	208.5	234.0

a Distortion spectra; b One band

The energy of electronic transitions depends strongly on the ligand field symmetry surrounding the molybdenum center. For oxo-ligands, a more energetic transition is expected for a tetrahedral Mo(VI) than for octahedral Mo(VI), Fournier et al (1989). The comparison of the electronic spectra obtained for SoMo and AHM solutions revealed a greater difference in the shift of the main band of the former solutions when the Mo concentration was increased. The difference was found at 5 nm (0.138 eV) and 9.5 nm (0.259 eV), respectively, although a greater difference (28.5 nm - 0.715 eV) can be seen if the main band at 250 ppm is taken into consideration. Nevertheless, the differences between the tetrahedral and octahedral species in aqueous media were quite small. Thus, an overlapping of the bands in the electronic spectra of the tetrahedral and octahedral species is expected to occur. For both solutions the largest difference observed was 4 nm (0.106 eV).

Figure 4 shows the DR spectra for Mo/Al_2O_3 samples prepared from AHM solutions in the oxidized (MoO_3) and impregnated (AHM ion) states. The spectrum of the MoO_3/Al_2O_3 exhibits a strong adsorption, with a maximum at 247.5 nm, similar to that of the dry impregnates exhibiting bands at 244.5 and 243 nm. The shape of the spectra was similar for all the samples. The absorption band has the typical shape of Mo(VI) species, Lutra & Cheng (1987), Xiong *et al*. (2000), Fournier *et al*. (1989). Since the Mo(VI) ion has a d0 electronic configuration, the only absorption band that is able to arise in the UV-Vis range of the electronic spectra comes from ligand-metal charge transfer. This band type is usually observed between 200 and 400 nm. However, since the alumina itself exhibits a broad band at 200-350 nm, the resulting spectra of the MoO_3/Al_2O_3 systems could be considered as the overlap of the adsorption bands at 225, 275 and 300 nm. The resulting broad band suggests that both molybdate species were developed in the wet state on the alumina surface. After drying and calcination, the band is still broad, suggesting the formation of some surface polymerized molybdate species. This inference is consistent with the observations of Fournier *et al*. (1989) and Ramirez *et al*. (1999).

The DR spectra for AHM and SoMo salt precursors only exhibit the characteristic wavelength bands for octahedral and tetrahedral species respectively, van Veen *et al*. (1987, 1990), Lutra & Cheng (1987), Hachiya *et al*. (1984), Gajardo *et al*. (1980), Fournier *et al*. (1989). There were larger differences in the intensity and wavelength positions for the octahedral and tetrahedral symmetries, due to different interactions between the Mo atoms and their surroundings, this it is related with the structure of MoO_3 and its crystal faces obtained by molecular modeling, Gesarai *et al* (1997).

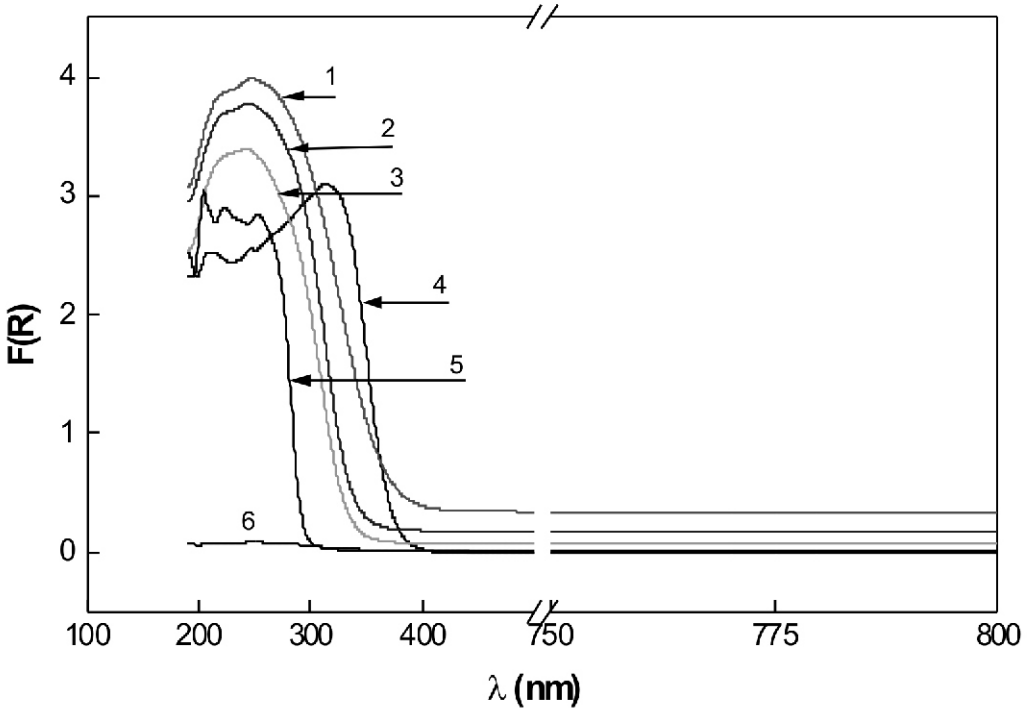

Figure 4. DRS-Uv-Vis spectra of Mo/alumina samples: (1) MoO_3/γ-Al_2O_3; (2) AHM/γ-Al_2O_3, rotary evaporator dried; (3) AHM/γ-Al_2O_3, dried naturally; (4) AHM salt; (5) SoMo salt; (6.), Γ-Al2O3 (AK) support.

The analysis of the reflectance spectra using model compounds confirmed that both type species (octahedral and tetrahedral) were present in the impregnates. Although most octahedral species were in solution, a small proportion of monomeric MoO_4^{-2} species always remained in equilibrium with the heptamer (Eq. 1), which may also lead to adsorption on the surface as minor species, Jiang *et al*. (2008) and Weigold (1983). Finally, we found that the hydration degree and the type of drying (RD, rotary dry; ND, natural dry) did not change the DR spectra, and exerted a negligible effect on the absorption bands of AHM/Al_2O_3 sample. Thus, as already reported by Fournier *et al*. (1989), the structure of the adsorbed species should not change.

3.1.2 Co and/or Pt on γ-Al_2O_3 or MoO_3/γ-Al_2O_3 systems

A similar behavior was observed for the adsorption of cobalt and platinum ions on the MoO_3/γ-Al_2O_3 surface. Under the experimental conditions used, most ionic species in solution were Pt (IV) and Co(II), in agreement with the work of Regalbuto et al. (1999) for Pt, and of Tamura et al. (1997) and Bergwerff et al. (2008) for Co ions. Also, the UV-Vis spectra for cobalt solutions (not shown here) were essentially the same as those reported by Tomisic & Simeon (1999). However, the initial pH of the impregnating H_2PtCl_6 solutions was lower than that reported by Ruckenstein & Karpe (1989) for Pt ions. The general equations for complete dissociation of the salts in aqueous medium are:

$$H_2PtCl_6 \Leftrightarrow 2H^+ + PtCl_6^{2-} \quad (2)$$

$$Co(NO_3)_2 \Leftrightarrow 2\,NO_3^- + Co^{2+} \quad (3)$$

For ensuring the adsorption equilibrium had been reached, each point of the adsorption isotherm (298 K) was extended for a much longer time (24 h). As pointed out in the previous section, the adsorption of ions on the alumina surface led to significant changes in the pH of the impregnating solution. The results offered in Table 1 indicate that the initial solution pH for most solutions

shifted to values close to the point of zero charge of the support (γ-Al_2O_3 or MoO_3/γ-Al_2O_3) at the end of impregnation. For a given support, the final pH values were in general higher than the initial pH for the impregnation of Pt on MoO_3/γ-Al_2O_3 and Pt-Co on MoO_3/γ-Al_2O_3, while pH was lower for the impregnation of Co on MoO_3/γ-Al_2O_3. This observation is consistent with the close proximity of the final pH solution and the point of zero charge of (pH_{ZPC}) of the molybdena support at the adsorption equilibrium. It should be noted that the final pH values of the impregnating solutions approached the pH_{ZPC} of the solid (MoO_3/γ-Al_2O_3 and γ-Al_2O_3). These results are in complete agreement with the pH_{ZPC} values reported by Kohler et al. (1992) for MoO_3/Al_2O_3 system and with those of Tawei *et al*. (1997) for γ-Al_2O_3. A final remark is that for the concentration limit of Co(II) ions, the pH values are lower than expected.

3.2 Adsorption isotherms

The adsorption isotherms of molybdenum (cobalt and platinum) at a constant temperature of 298 K, expressed as the amount of metal ion retained per gram of solid (C_a) as a function of the metal ion concentration of the impregnating solution at equilibrium (C_{eq}), were determined. The experimental isotherms for the different supports are shown in (Figs. 5-11.) The isotherms for the metal ion/γ-Al_2O_3 systems belong to the L-type of the Giles classification, Giles et al. (1974). Exceptions were the isotherms obtained using CoAc and CoCl salt precursors and a PR alumina (Fig. 10), and also Pt (Co) on MoO_3/alumina (Fig. 11).

For the adsorption of molybdate ions, the shape of the isotherms (Figs. 5 and 6) coincides with that reported in the literature for this system, Al-Dalama *et al*. (2005), Bourikas *et al*. (1998), Pizzio *et al*. (1996), van Veen *et al*. (1987), Mulcahy *et al*. (1987). However, depending on the range of C_{eq} values investigated, the shape of these isotherms may vary. Thus, more complex shapes can be found, particularly if the isotherm covers a broad range of Ceq concentrations, Vissenberg et al. (2000), Bourikas *et al*. (1996, 1998, 2006). Ca values increased rapidly with C_{eq} in the range of concentrations up to ca. 15 mg/ml and 5 mg/ml for the AHM and SoMo solutions, respectively, whereas the curves flattened off at higher concentrations. An important distinction among the three γ-Al_2O_3 supports is that, whatever the concentration, higher amounts of Mo were retained by the γ-Al_2O_3 (AK) sample. Moreover, the experimental isotherms determined using the impregnating SoMo salt precursor clearly shows up the differences in the adsorption capability of the three γ-Al_2O_3 substrates. In this case, the sequence in adsorption capability was AK >> RO >> PR alumina. The adsorption capacity was highest when AHM salt was used as the impregnating solution, in which case the sequence was AK >> RO > PR.

The adsorption behavior is influenced by the surface properties of the alumina (adsorption sites, IEP and/or ZPC) and the solution characteristics (pH and nature of the ionic species), Lutra & Chang (1987), Mestl & Srinivasan (1998), Semagina & Kiwi-Minsker (2009). On the basis of these characteristic properties, an explanation of the differences found between the adsorption of AHM (octahedral species) and SoMo (tetrahedral) salt precursors can be offered. The AK-type alumina must have a higher affinity for octahedral than for tetrahedral species because the AK alumina showed a higher experimental S (mg ion/g support) value. By contrast, a poor affinity of the surface for tetrahedral molybdate species was reflected in the adsorption from SoMo solutions in which only tetrahedral MoO_4^{2-} species, but in no case octahedral $Mo_7O_{24}^{6-}$ units, are present. The RO and PR alumina samples showed a similar kind of behavior. Upon observing the adsorption isotherms in (Figs. 5 and 6), it appears that the RO and PR γ-Al_2O_3 substrates would have similar proportions of adsorption sites for the octahedral species, although still lower than for the PR counterpart. It should be stressed that specific area and porosity would have only a minor influence in the adsorption of molybdate ions.

A similar type of behavior was observed for the adsorption of Co(II) ions on alumina, see (Figs. 7-10), Bergwerff et al. (2008), Wang & Hall (1982), Bourikas et al. (1998), Siri et al. (1985). In all cases, the PR-type alumina had a slightly higher adsorption capacity than the other aluminas. There is, however, an interesting point to be considered in (Fig. 10); although the initial concentration was the same for all the experiments, C_{eq} values were very different at the end of the adsorption (a higher amount of Co(II) ions was adsorbed). Thus, PR-type alumina

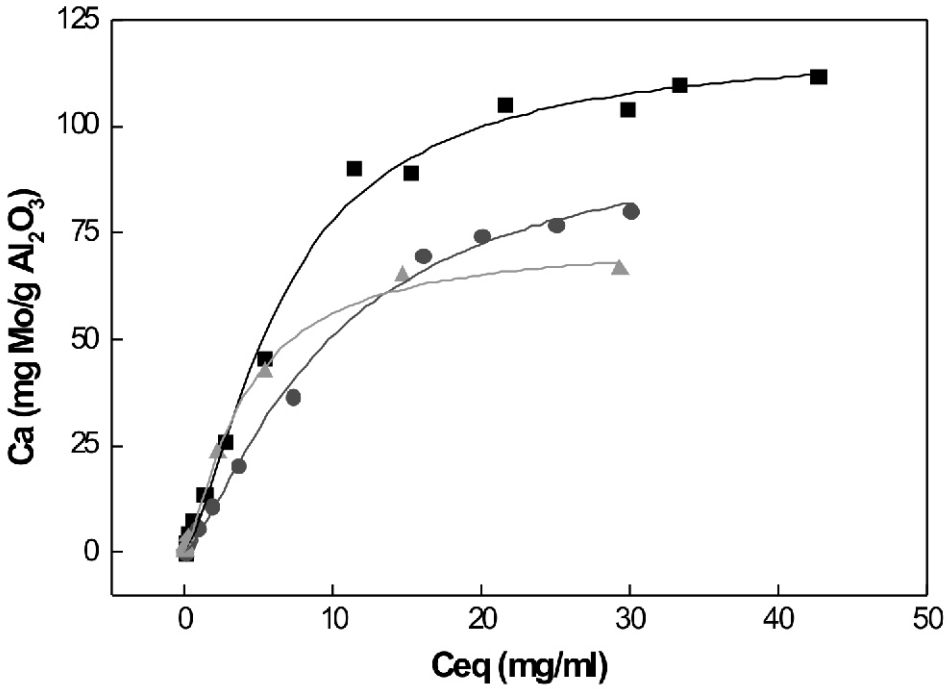

Figure 5. Room temperature adsorption isotherms of molybdenum (AHM) on alumina supports: (■) γ-Al_2O_3 (AK); (•) γ-Al_2O_3 (RO); (▲) γ-Al_2O_3 (PR). The lines represent the fitting of the experimental adsorption data to the isotherms derived from the equilibrium parameters.

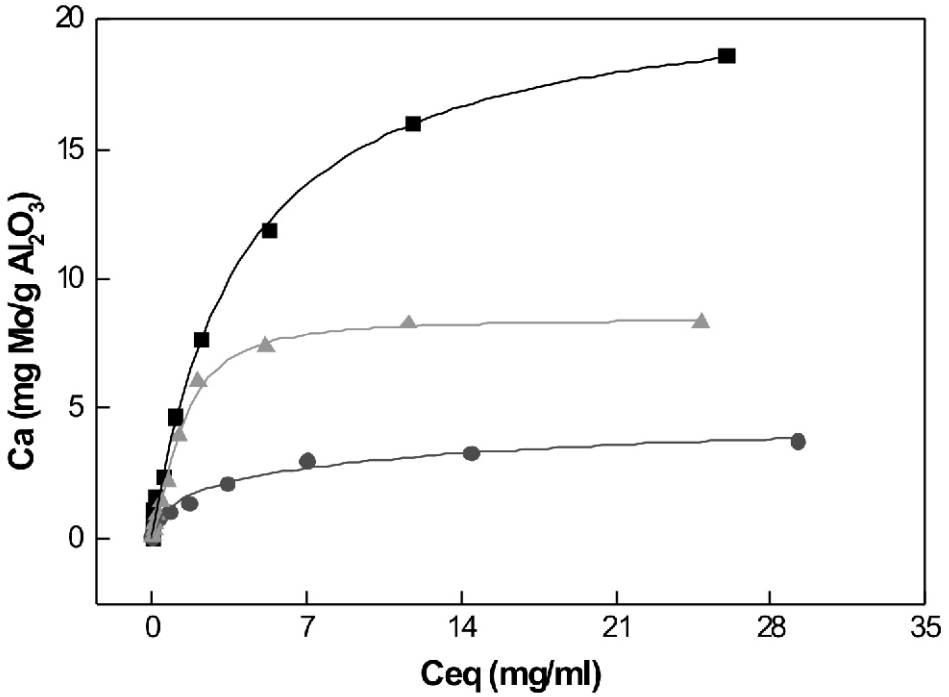

Figure 6. Room temperature adsorption isotherms of molybdenum (SoMo) on alumina supports: (■) γ-Al_2O_3 (AK); (•) γ-Al_2O_3 (RO); (▲) γ-Al_2O_3 (PR). The lines represent the fitting of the experimental adsorption data to the isotherms derived from the equilibrium parameters.

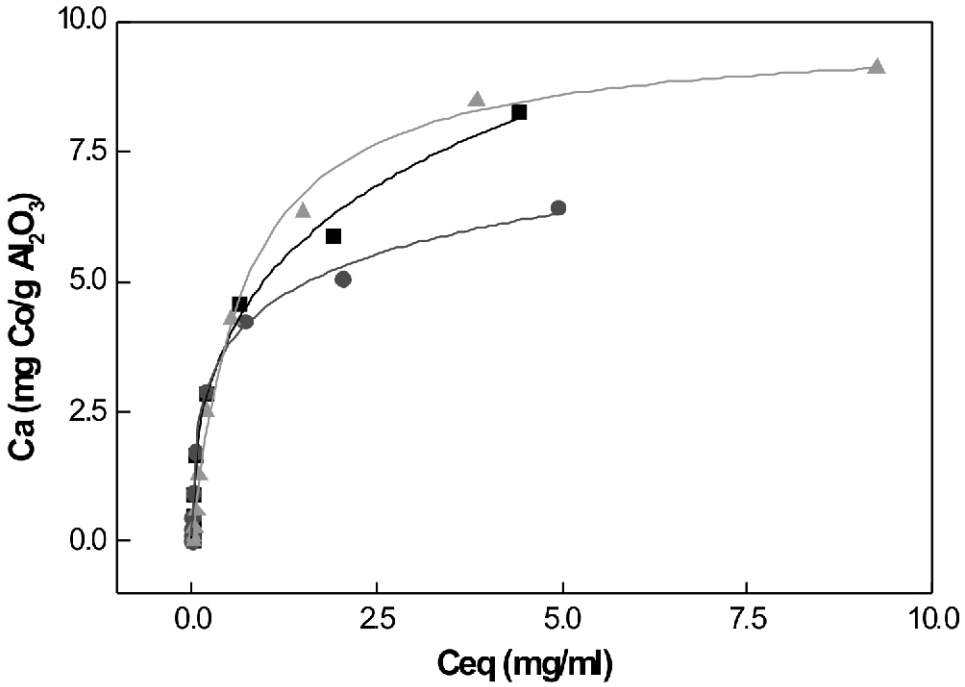

Figure 7. Room temperature adsorption isotherms of cobalt (CoNi) on alumina supports: (■) γ-Al_2O_3 (AK); (•) γ-Al_2O_3 (RO); (▲) γ-Al_2O_3 (PR). The lines represent the fitting of the experimental adsorption data to the isotherms derived from the equilibrium parameters.

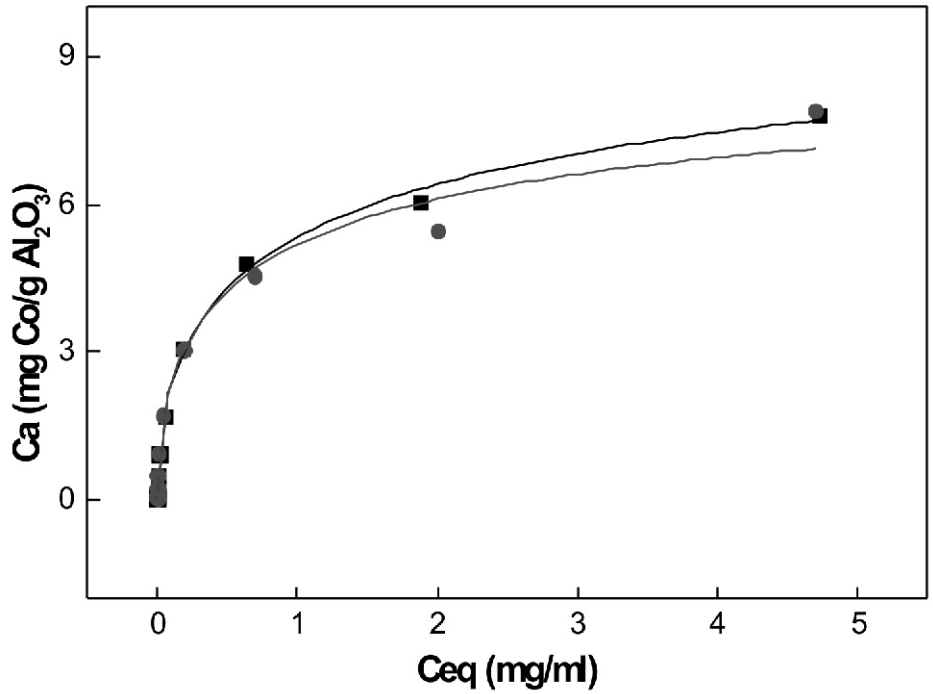

Figure 8. Room temperature adsorption isotherms of cobalt (CoCl) on alumina supports: (■) γ-Al_2O_3 (AK); (•), γ-Al_2O_3 (RO). The lines represent the fitting of the experimental adsorption data to the isotherms derived from the equilibrium parameters.

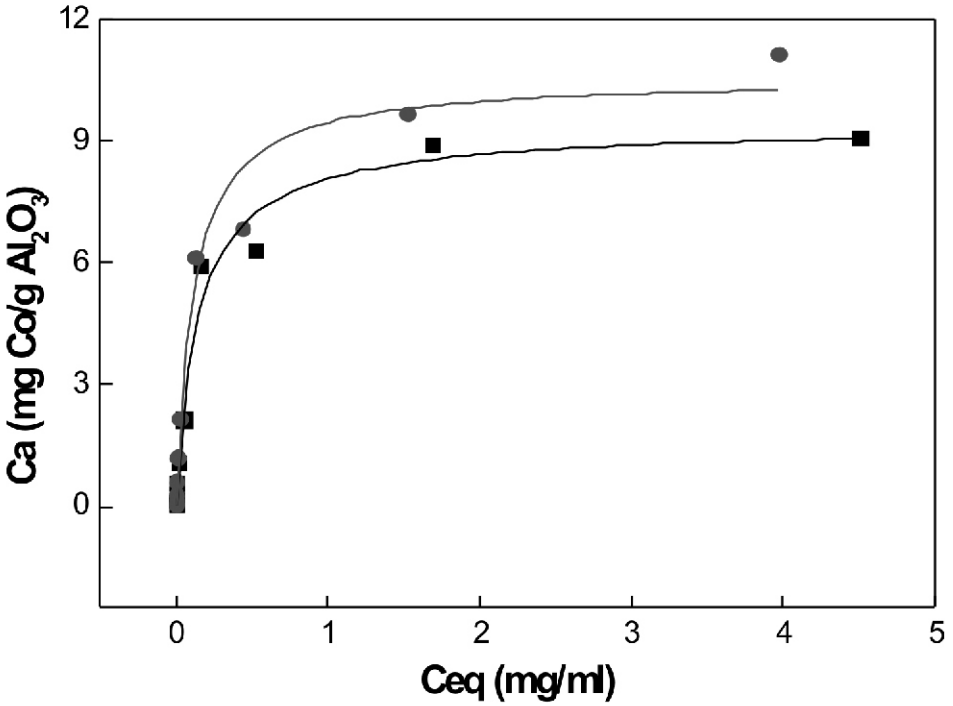

Figure 9. Room temperature adsorption isotherms of cobalt (CoAc) on alumina supports: (■) γ-Al_2O_3 (AK); (•) γ-Al_2O_3 (RO). The lines represent the fitting of the experimental adsorption data to the isotherms derived from the equilibrium parameters.

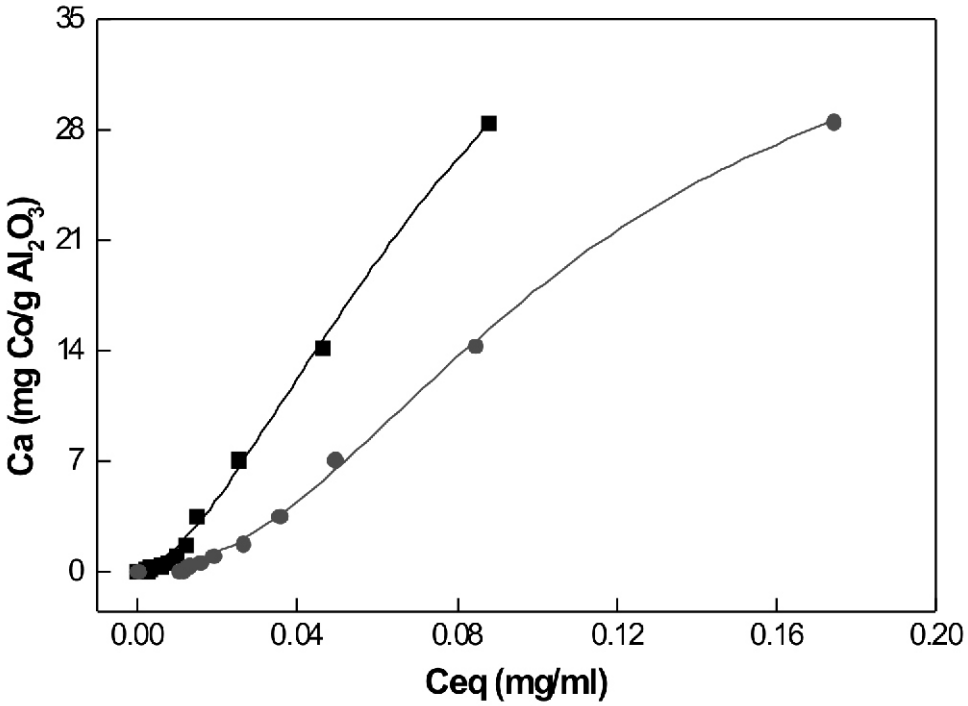

Figure 10. Room temperature adsorption isotherms of cobalt on γ-Al_2O_3 (PR): (■) CoAc; (•) CoCl. The lines represent the fitting of the experimental adsorption data to the isotherms derived from the equilibrium parameters.

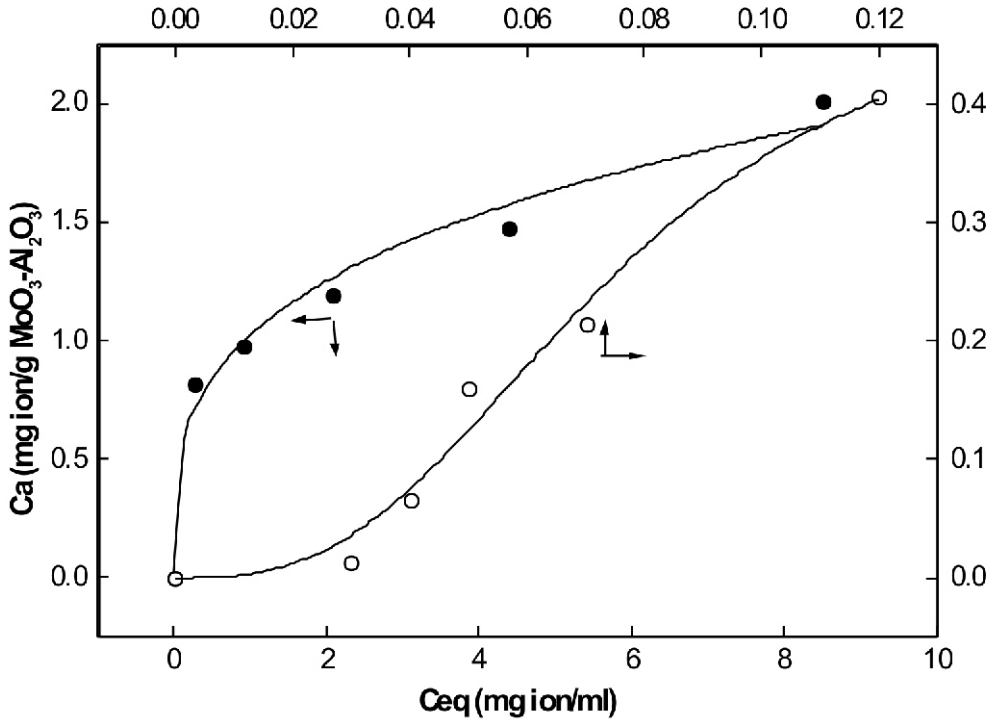

Figure 11. Room temperature adsorption isotherms of platinum and cobalt ions on MoO_3/ γ-Al_2O_3 (AK): (•), Co (Pt); (○), Pt (Co). The lines represent the fitting of the experimental adsorption data to the isotherms derived from the equilibrium parameters.

exhibited a higher adsorption capacity than the AK and RO counterparts. Since these gave rise to an S-type shaped isotherm within the concentration range used, differences in impurity levels and in surface chemical groups of each alumina could well be responsible for this behavior. The curve shape found for CoNi, CoCl and CoCl adsorption suggests that the adsorption sites in the AK y RO alumina are similar.

The adsorption isotherms of Co (Pt) and Pt (Co) on MoO_3/γ-Al_2O_3 are shown in (Fig. 11). The isotherm for Pt (Co) belongs to the S-type; this shape is very different from the L type, which was found for the Pt adsorption on MoO_3/Al_2O_3, Machuca et al (2001). The presence of Co(II) ion in solution may alter both the kinetics and extent of Pt adsorption. Similarly, the Co adsorption on MoO_3/alumina changed when Pt ion was also present in solution. In this case, the shape of the isotherm was of the L-type, which differs from the S-type found for the adsorption of Co(II) ions on MoO_3/alumina. In a previous work, Machuca et al (2001), it was observed that adsorbed, irrespective of the Al_2O_3 source used the adsorption sites on MoO_3/γ-Al_2O_3, where the ionic species (Co(II) or Pt(IV)) were adsorbed, can be virtually the same in each case since the new surface is the MoO_3 oxide deposited over the Al_2O_3 substrate.

The observed behavior can be explained in terms of the two types of isotherms (S and L), which imply lateral interactions between the Pt(IV) and Co(II) species in solution. As a consequence, the equilibrium adsorption capacity of the MoO_3/Al_2O_3 surface may be modified by these interactions. In this sense, a reduction in the Co(II) ion adsorption capacity on MoO_3/alumina surface was observed when Pt(IV) ions were in solution and vice versa. Within the concentration range used, the equilibrium adsorption capacity ratio (with and without ions) was 8/1 and 13/4 for the Co and Pt, respectively. This different behavior can be explained in terms of the equilibrium distribution of adsorbate species between the surface of the support and the liquid phase, which depends on the concentration and nature of the ions, temperature, the chemical nature

of the support and the interface (liquid-solid) and ion-ion interactions, Giles *et al*. (1974). Consequently, when more than one adsorbate is present in solution, the interaction between different ions for the adsorption sites must be taken into account.

This assumption is reinforced by the observation that Co(II) and Pt(IV) ions will interact electrostatically with a molybdate phase bound to the surface. As a consequence of the simultaneous participation of the three species, the adsorption process is more complex. Since an S-type shaped isotherm was found within the concentration range used, this reflects the additive effect of the incorporated ion. Noble metal (Pt,Ru,Pd)-Mo/alumina samples prepared by Meriño et al. (2000) showed a decrease in the activity for the hydrodesulfurization reaction of dibenzothiophene when one monolayer of the MoO_3-like phase was developed on the alumina substrate and, subsequently, Pt(IV) ions were adsorbed on the MoO_3/Al_2O_3 system. However, a better activity of the catalysts can be obtained by keeping the Mo-loading below the monolayer capacity of the Al_2O_3 surface, Pinzon et al. (2006), Giraldo *et al*. (2008), these results confirm that both the monolayer of Mo species on the surface and the ion coimpregnation influence the adsorption process during the impregnation steps of noble metal-Mo/alumina samples.

In addition, Spanos & Lycourghiotis (1994) have reported that mutual promotion exists in the adsorption of Mo(VI) and Co(II) ion species on Al_2O_3 in the 4.1-6.1 pH range; this was attributed to the strong lateral interactions exerted between Mo(VI) and Co(II) ions in solution. Finally, most of the adsorption isotherms for $PtCl_6^{2-}$ ions reported in literature correspond to the Pt/Al_2O_3 system, Lee & Aris (1985), Gavriilidis *et al*. (1993), for which the effects of several inorganic and organic acids as competing agents on the deposition of Pt on alumina have been extensively investigated. Thus, Gavriilidis *et al*. (1993) and Papageorgiou *et al*. (1996) have reported the use of the modified Langmuir model to quantitatively describe transient adsorption studies of the Pt-citric acid system, which in turn also accounted for the effects of the solution and steric hindrance.

3.3 Numerical Calculations

For the quantitative description of the above isotherms, numerical calculations were carried out. For this purpose, different equations relating the equilibrium concentration in solution and the amount of adsorbed species were examined, Bourikas et al. (1996, 2006), Giles *et al*. (1974), Ruthven (1984). In this sense, the main goal was to obtain an expression or relationship that could be easily used to model the impregnation steps and to predict the concentration profile of the active component inside the pellet. The classic Langmuir expression was taken as the starting point for these studies. The Langmuir equation establishes a relationship between Ca and C_{eq} by:

$$Ca_{eq} = \frac{K_e.S.C_{eq}}{1 + K_e.C_{eq}} \tag{4}$$

where K_e (ml/mg) is the equilibrium adsorption constant; S (mg ion/g support) is the corresponding surface concentration at equilibrium, and C_{eq} (mg/ml) is the solution concentration.

Other expressions such as those proposed by Giles, Kitchener, Henry and Freundlich were also used to quantitatively describe the relationship between Ca and C_{eq}, Pizzio *et al*. (1996), Giles *et al*. (1974), Ruthven (1984), Bearing in mind the assumption of these authors for type S isotherms, the expressions for Giles and Kitchener are:

$$Ca_{eq} = \frac{K_G.S.C_{eq}^{x}}{1 + K_G.C_{eq}^{x}} \tag{5}$$

$$Ca_{eq} = \frac{K_1.S.C_{eq}10^{-k1\theta}}{1 + K_1.C_{eq}10^{-k1\theta}} \tag{6}$$

Where K_G (ml/mg)x is the Giles equilibrium adsorption constant, S is the saturation concentration (mg ion/g support) at equilibrium; x is an exponential that describes the isotherm shape; K_1 and k_1 are constants, and θ= Ca/S is the fraction of adsorption sites occupied. The Giles and Kitchener expressions are related to the Lagmuir constant by $Ke=K_GC_{eq}^{x-1}$ and $Ke=K_110^{-k1\theta}$ respectively.

Using a non-linear least-squares algorithm (Levenberg-Marquart), the equilibrium adsorption parameters for each system and equation were calculated from the fitting of the equilibrium data. This procedure was accomplished by minimizing the χ^2 parameter. The group of parameters showing the best fit to the experimental isotherm is summarized in the (Table 3). Although in most cases the difference between the equations is very small, the choice basically depends on the simplicity of the mathematical model chosen to describe the impregnation process.

From Figs. 5 and 6 and Table 3, it is clear that the γ-Al_2O_3 (AK) sample shows a slightly higher adsorption capacity than its γ-Al_2O_3 (RO and PR) counterparts for Mo ion adsorption, although this difference is clearer in the SoMo isotherm. All the γ-Al_2O_3 samples studied exhibited a higher affinity for polymeric molybdate than for monomeric ions. This difference may be due to the presence of different impurities and the different amount and types of sites for adsorption (hydroxyl types) on those surfaces, since the textural parameters and pH_{ZPC} values are very close, Giordano et al. (1975), Adachi et al. (1996). The γ-Al_2O_3 (AK) sample has a higher S (mg Mo/g alumina) value than its γ-Al_2O_3 (RO and PR) counterparts.

At low concentration values, up to 5 mg/mL, the isotherms show a Henry-type behavior. Thus, the Henry constant for the AK-type Al_2O_3 sample is higher than for the RO- and PR-type γ-Al_2O_3 counterparts. This observation again suggests a higher availability of adsorption sites on the AK-type γ-Al_2O_3 than on the RO- and PR-type γ-Al_2O_3 surfaces.
The fitting parameters, the saturation coverage of Mo, and the equilibrium constant, calculated from the Giles, Langmuir and Freundlich model are

Table 3. Equilibrium adsorption parameters derived from the fittings

System	Giles				Langmuir			Freundlich		
	K_G	S	X	χ^2	Ke	S	χ^2	A	B	χ^2
AHM/Al_2O_3 (AK)	0.0658	119.00	1.45	15.50	0.109	140	25.50	22.75	0.455	110
AHM/Al_2O_3(RO)	0.0481	100.00	1.32	4.09	0.059	130	6.11	10.58	0.622	19.2
AHM/Al_2O_3(PR)	0.1692	73.27	1.28	2.62	0.209	80	3.15	18.550	0.408	25.6
SoMo/Al_2O_3(AK)	0.2460	23.26	0.87	0.18	0.253	21	0.20	5.249	0.411	1.07
SoMo/Al_2O_3(RO)	0.2780	5.99	0.55	0.02	0.393	3.9	0.05	1.308	0.335	0.04
SoMo/Al_2O_3(PR)	0.6670	8.50	1.49	0.07	0.579	9.4	0.20	3.070	0.366	1.63
CoNi/Al_2O_3 (AK)	0.2140	28.62	0.41	0.03	2.380	8.2	0.32	4.899	0.353	0.04
CoNi/Al_2O_3(RO)	0.5960	12.05	0.38	0.01	5.838	5.9	0.25	4.260	0.270	0.04
CoNi/Al_2O_3(PR)	1.3760	9.88	0.97	0.05	1.431	9.7	0.05	4.392	0.383	1.03
CoCl/Al_2O_3(AK)	0.7720	12.22	0.51	0.02	3.654	7.5	0.20	4.913	0.319	0.12
CoCl/Al_2O_3(RO)	1.1180	9.83	0.55	0.17	3.359	7.3	0.42	4.784	0.310	0.10
CoCl/Al_2O_3(PR)	92.300	39.63	2.04	0.10	-	-	-	252.0	1.231	1.43
CoAc/Al_2O_3 (AK)	5.8950	9.45	0.92	0.29	7.338	9.2	0.26	6.680	0.294	1.25
CoAc/Al_2O_3(RO)	1.9430	13.63	0.56	0.21	8.636	10	0.49	8.142	0.280	0.63
CoAcl/Al_2O_3(PR)	47.820	58.87	1.61	0.18	-	-	-	547.6	1.210	0.53
Co-(Pt)/MoO_3/Al_2O_3 (AK)	-	-	-	-	1.426	1.9	0.06	1.023	0.291	0.01
Pt-(Co)/MoO_3/Al_2O_3(AK)	1535.8	0.51	2.82	7E-4	-	-	-	8.144	1.403	1E-3

shown in Table 3. The close values of x (1.45, 1.32 and 1.28 for AHM adsorption) indicate that the shape of the curves is quite similar for all three aluminas. There are differences between the SoMo isotherms on alumina, reflected in the parameter values. These results lie in the same range as many others reported in the literature. At this juncture it should be emphasized that the reported values for S and K_e (Langmuir model) for the adsorption of molybdenum on alumina surfaces are scattered over broad ranges. Thus, Mo saturation coverages from 50 to 156 mg Mo/g alumina and adsorption equilibrium constants from 1.9 x 10-4 to 1.65 ml/mg Mo can be found in the literature, van Veen et al. (1987), Giles et al. (1974), Gavriilidis et al. (1993), Pizzio et al. (1996). Although the chemical properties associated with the presence of different levels of impurities may alter the proportion of adsorption sites, textural properties may also contribute to exacerbating the observed differences.

Table 3 and Figs. 7-10 show that the Co/γ-Al_2O_3 systems display almost identical L-shaped isotherms, except for CoAc and CoCl adsorptions on PR alumina, which exhibit an S type. This type of behavior suggests that either the same type of adsorption sites for Co are available on the γ-Al_2O_3 surface or that a similar deposition process is operative along the impregnation and drying steps, irrespective of the second ion in solution. For PR-type alumina and CoCl and CoAc systems, the Langmuir model obviously did not apply; however, the Giles equation revealed an appropriate fitting of the adsorption data. Within the C_{eq} concentration range explored, a stronger adsorption of Co(II) ions on PR-type alumina than for the other two aluminas was found.

By contrast, the two Pt(Co)/MoO_3/γ-Al_2O_3 and Co(Pt)/MoO_3/γ-Al_2O_3 samples showed the opposite adsorption behavior. The data can be satisfactorily described by the Freundlich and Giles equations respectively (Fig. 11 and Table 3). Saturation values of 2.0 mg Co/g MoO_3-Al_2O_3 and 0.4 mg Pt/g MoO_3-Al_2O_3 for the AK-type substrate were derived from the fitting. These values are lower than the adsorption data reported for Pt/γ-Al_2O_3 catalysts. This monometallic system showed values between 21 to 56 mg Pt/g Al_2O_3 (110-290 μmol H_2PtCl_6/g Al_2O_3) and 0.56 to 159 ml/mg Pt (110-31000 l/mol H_2PtCl_6) for the surface saturation coverage and the equilibrium adsorption constant, K_e, respectively, Lee & aris (1985), Papageorgiou et al. (1996). The large difference observed in the saturation values for Pt can be explained in terms of the notion that most of the adsorption sites are located on the alumina surface, and in turn disappear upon molybdenum incorporation and interaction with the ion in solution. Some discrepancies may also arise from the experimental conditions of the impregnation process used in the adsorption step.

4. Conclusions

The extent of Mo adsorption on the γ-Al_2O_3 surface depended on the type of molybdate species (tetrahedral and octahedral) in solution. Moreover, the adsorption process suggested that polymeric and monomeric species are present in the wet, dry and calcined states, since surface groups and alumina impurities can modify the adsorption process. The γ-Al_2O_3 (AK) sample showed a slightly higher adsorption capacity for Mo than its γ-Al_2O_3 (RO and PR) counterparts. At low concentration values (until 5 mg/ml), the Mo isotherms were almost linear (Henry-type behavior), with the Henry constant for the Al_2O_3 (AK) higher than for the other γ-Al_2O_3. This observation suggests a higher availability of adsorption sites on the γ-Al_2O_3 (AK) than on the γ-Al_2O_3 (RO and PR) surface.

For Co systems, it was observed that: (a) for Co adsorption, the same sites are present on the alumina surface when different precursors are used; (b) the shape of the adsorption isotherm of Pt on MoO3/γ-Al_2O_3 surface changes from the S- to the L-type; (c) since L- and S-shaped isotherms were found for the Co/γ-Al_2O_3 and Co-MoO_3/γ-Al_2O_3 systems respectively, the adsorption of Co species was altered by the MoO_3/γ-Al_2O_3 substrate.

5. Acknowledgements

Machuca-Martinez gratefully acknowledges COLCIENCIAS, UIS and UNIVALLE (Colombia) and ICP-CSIC (Spain) for a fellowship and financial support. The alumina supports used in the present work were kindly supplied by Akzo-Nobel (The Netherlands), Rhodia (France) and Procatalyse (France).

6. References

Achchar, M., Lamonier, C., Ezzamarty, A., Lakhdar, M., Leglise, J., & Payen, E. (2009). New apatite-based supports prepared by industrial phosphoric acid for HDS catalyst synthesis. *Comptes Rendus Chimie* 12 (6-7), 677-682.

Adachi, M., Contescu, C., & Schwarz, J. A. (1996). The Use of Proton Affinity Distributions for the Characterization of Active Sites of Alumina-Supported Co-Mo Catalysts. *Journal of Catalysis* 158 (2), 411-419.

Al-Dalama, K., Aravind, B., & Stanislaus, A. (2005). Influence of complexing agents on the adsorption of molybdate and nickel ions on alumina. *Applied Catalysis A-General* 296 (1), 49-53.

Baumgarten, E., & Kirchhausen-Dusing, U. (1997). Sorption of Metal Ions on Alumina. *Journal of Colloid and Interface Science* 194 (1), 1-9.

Bejenaru, N., Lancelot, C., Blanchard, P., Lamonier, C., Rouleau, L., Payen, E., Dumeignil, F., & Royer, S. (2009). Synthesis, Characterization, and Catalytic Performances of Novel CoMo Hydrodesulfurization Catalysts Supported on Mesoporous Aluminas. *Chemistry of materials* 21 (3), 522-533.

Baldovino-Medrano, V.G., Giraldo, S.A., & Centeno, A. (2009). The functionalities of Pt-Mo catalysts in hydrotreatment reactions, Fuel, In Press, DOI: 10.1016/j.fuel.2009.12.002.

Bergwerff, J.A., Visser, T., & Weckhuysen, B.M. (2008). On the interaction between Co- and Mo-complexes in impregnation solutions used for the preparation of Al2O3-supported HDS catalysts: A combined Raman/UV-vis-NIR spectroscopy study. *Catalysis Today* 130 (1), 117-125.

Bourikas, K., Goula G.A., & Lycourghiotis, A. (1998). Kinetics of Deposition of the Mo−Oxo Species on the Surface of γ-Alumina. *Langmuir* 14 (17), 48194826.

Bourikas, K., Kordulis, C., & Lycourghiotis, A. (2006). The Role of the Liquid-Solid Interface in the Preparation of Supported Catalysts. *Catalysis Reviews Science and Engineering* 48 (4), 363 - 444.

Bourikas, K., Matralis, H.K., Kordulis, Ch., & Lycourghiotis, A. (1996). Mechanisms of Deposition of Species Containing Catalytically Active Ions on the Oxidic Support/Electrolytic Solution Interfaces: A Unified Approach Based on the Two-pk/One-Site and Triple-Layer Models. *Journal of Physical Chemistry* 100 (28), 1171111719.

Butz, T., Vogdt, C., Lerf, A., & Knözinger, H. (1989). Time differential perturbed angular correlation of γ-rays emitted from $^{99}Mo \rightarrow {}^{99}Tc$ in molybdenum-based catalysts : The nature of molybdate species in molybdena/alumina catalysts. *Journal of Catalysis*, 116 (1), 31-48.

Chianelli, R.R., Berhault, G., & Torres, B. (2009). Unsupported transition metal sulfide catalysts: 100 years of science and application. *Catalysis Today* 147 (3-4), 275-286

Chu, T. W., Du J. Z., & Tao., Z. Y. (1997). Adsorption of H^+, OH- and Background Electrolyte Ions on Alumina-point of Zero Charge, Triple Layer Model (TLM) Parameters and Thermodynamic Parameters. *Adsorption Science and Technology* 15 (1), 455-463

De Lacaillerie, JBD., & Gan, Z. (2007). MAS NMR strategies for the characterization of supported molybdenum catalysts. *Applied magnetic resonance* 32 (4), 499-511.

de Wilmar, D. M., & Clause, O. (1998). Adaptation of 27Al CP/MAS NMR to the Investigation of the Adsorption of Molybdate Ions at the γ-Al_2O_3/Water Interface. *Journal of Physical Chemistry* B 102 (36), 70237027.

Duan, A.J., Wan, G.F., Zhao, Z., Xu, C.M., Zheng, Y.Y., Zhang, Y., Dou, T., Bao, X.J., & Chung, K. (2007). Characterization and activity of Mo supported catalysts for diesel deep hydrodesulphurization. *Catalysis Today* 119 (1-4), 13-18.

Eliche-Quesada, D., Rodriguez-Castellon, E., & Jimenez-Lopez, A. (2007). Hydrodesulfurization activity over supported sulfided ruthenium catalysts. Influence of the support, *Microporous and Mesoporous Materials* 99 (3), 268-278.

Fournier, M., Louis, C., Che, M., Chaquin, P., & Masure, D. (1989). Polyoxometallates as models for oxide catalysts : Part I. An UV-visible reflectance study of polyoxomolybdates: Influence of polyhedra arrangement on the electronic transitions and comparison with supported molybdenum catalysts. *Journal of Catalysis* 119 (2), 400-414.

Frizi, N., Blanchard, P., Payen, E., Baranek, P., Rebeilleau, M., Dupuy, C., & Dath, JP. (2008). Genesis of new HDS catalysts through a careful control of the sulfidation of both Co and Mo atoms: Study of their activation under gas phase. *Catalysis Today* 130 (2-4), 272-282.

Gajardo, P., Grange, P., & Delmon, B. (1980). Structure of oxide CoMo/[gamma]-Al203 hydrodesulfurization catalysts: An XPS and DRS study. *Journal of Catalysis* 63 (1), 201-216.

Gavriilidis, A., Varma, A., & Morbidelli, M. (1993). Optimal distribution of catalyst in pellets. *Catalysis Reviews - Science and Engineering* 35 (3), 399-456.

Gesari, S., Irigoyen, B., & Juan, A. (1997). Estudio estructural del MoO3 y sus planos cristalinos. *Quím. Nova* 20 (1), 99-102.

Giles, C. H., Smith, D., & Huitson, A. (1974). A general treatment and classification of the solute adsorption isotherm. I. Theoretical, *Journal of Colloid and Interface Science* 47 (3), 755-765.

Giordano, N., Bart, J. C. J., Vaghi, A., Castellan, A., & Martinotti, G. (1975). Structure and catalytic activity of MoO_3 [middle dot] Al_2O_3 systems : I. Solid-state properties of oxidized catalysts. *Journal of Catalysis* 36 (1), 81-92.

Giraldo, S.A., Pinzon, M.H., & Centeno, A. (2008). Behavior of catalysts with rhodium in simultaneous hydrodesulfurization and hydrogenation reactions. *Catalysis Today* 133 (1), 239-243.

Griboval, A., Blanchard, P., Payen, E., Fournier, M., & Dubois, J.L. (1998). Alumina supported HDS catalysts prepared by impregnation with new heteropolycompounds. Comparison with catalysts prepared by conventional Co-Mo-P coimpregnation. *Catalysis Today* 45 (1-4), 277-283.

Hachiya, K., Sasaki, M., Saruta, Y., Mikami, N., & Yasunaga, T. (1984). Static and kinetic studies of adsorption-desorption of metal ions on a gamma.-alumina surface. 1. Static study of adsorption-desorption. *Journal Physical Chemistry* 88 (1), 2327.

Iannibello, A., & Mitchell, P.C.H. (1979). Preparative Chemistry of Cobalt-Molybdenum/Alumina Catalysts. *Studies in Surface Science and Catalysis*, 3, 469-478

Jiang, Z., Huang, W., Zhao, H., Zhang, Z., Tan, D., & Bao, X. (2008). Preferential occupation of molybdenum on the thin alumina film: Characterization by CO titration. *Catalysis Today*, 131 (1-4), 28-34.

Kim, D. S., Ostromecki, M., Wachs, I. E., Kohler S. D., & Ekerdt. J. G. (1995). Preparation and characterization of WO_3/SiO_2 catalysts. *Catalysis Letters* 33 (3-4), 209-212.

Klimova, T., Mendoza Vara, P., & Puente Lee, I. (2009). Development of new NiMo/[gamma]-alumina catalysts doped with noble metals for deep HDS, *Catalysis Today*, In Press, DOI: 10.1016/j.cattod.2009.08.003.

Klimova, T., Solis-Casados, D., & Ramirez, J. (1998). New selective Mo and NiMo HDS catalysts supported on Al_2O_3-MgO(x) mixed oxides. *Catalysis Today* 43 (1-2), 135-146.

Komiyama, M. (1985). Design and Preparation of Impregnated Catalysts. *Catalysis Reviews - Science and Engineering* 27 (2), 341 372.

Kubicka, D., & Kaluza, L. (2010). Deoxygenation of vegetable oils over sulfided Ni, Mo and NiMo catalysts. *Applied Catalysis A: General* 372 (2), 199-208.

Kubota, T., Rinaldi, N., Okumura, K., Honma, T., Hirayama, S., & Okamoto, Y. (2010). In situ XAFS study of the sulfidation of Co-Mo/B_2O_3/Al_2O_3 hydrodesulfurization catalysts prepared by using citric acid as a chelating agent. *Applied Catalysis A: General* 373 (1-2), 214-221.

Kurhinen, M., & Pakkanen, T.A. (2000). CoMo/alumina prepared from carbonyl precursors: DRIFT, TPR and HDS studies. *Applied Catalysis A: General* 192 (1), 97-103.

Lamonier, C., Martin, C., Mazurelle, J., Harle, V., Guillaume, D., & Payen, E. (2007). Molybdocobaltate cobalt salts: New starting materials for hydrotreating catalysts. *Applied Catalysis B: Environmental* 70 (1-4), 548-556.

Lee, S.Y., & Aris, R. (1985). The Distribution of Active ingredients in Supported Catalysts Prepared by Impregnation. *Catalysis Reviews - Science and Engineering* 27 (2), 207 340.

Luthra, N. P., & Cheng, W-C. (1987). Molybdenum-95 NMR study of the adsorption of molybdates on alumina. *Journal of Catalysis* 107 (1),154-160.

Machuca, F., Giraldo de Leon, S., Centeno, A., & Fierro, J. L. G. (2001). Pt- (and Co-) Promoted Molybdena-Alumina Catalysts: Analysis of the Impregnation Steps. *Journal of Colloid and Interface Science* 237 (2), 290-293.

Merino, L. I., Centeno, A., & Giraldo, S. A. (2000) Influence of the activation conditions of bimetallic catalysts NM-Mo/[gamma]-Al_2O_3 (NM=Pt, Pd and Ru) on the activity in HDT reactions. *Applied Catalysis A: General* 197 (1), 61-68.

Mestl, G.A, & Srinivasan, T.K.K. (1998). Raman spectroscopy of monolayer-type catalysts: Supported molybdenum oxides. *Catalysis Reviews - Science and Engineering* 40 (4), 451-570.

Navarro, R.M., Pawelec, B., Trejo, J.M., Mariscal, R., & Fierro, J. L. G. (2000). Hydrogenation of Aromatics on Sulfur-Resistant PtPd Bimetallic Catalysts. *Journal of Catalysis* 189 (1), 184-194.

Mulcahy, F. M., Houalla, M., & Hercules, D. M. (1987). The effect of the isoelectric point on the adsorption of molybdates on fluoride-modified aluminas. *Journal of Catalysis* 106 (1), 210-215.

Pashigreva, A. V., Klimov, O.V., Bukhtiyarova, G. A., Kochubey, D. I., Prosvirin, I. P., Chesalov, Y. A., Zaikovskii, V. I., & Noskov, A. S. (2009). High-active hydrotreating catalysts for heavy petroleum feeds: Intentional synthesis of CoMo sulfide particles with optimal localization on the support surface. *Catalysis Today* In Press, DOI: 10.1016/j.cattod.2009.08.021.

Papageorgiou, P., Price, D. M., Gavriilidis, A., & Varma, A. (1996). Preparation of Pt/[gamma]-Al2O3 Pellets with Internal Step-Distribution of Catalyst: Experiments and Theory. *Journal of Catalysis* 158 (2), 439-451.

Pinzon, M.H., Centeno, A., & Giraldo, S.A. (2006). Role of Pt in high performance Pt-Mo catalysts for hydrotreatment reactions. *Applied Catalysis A-General* 302 (1), 118-126.

Pizzio, L.R., Vázquez, P.G., Cáceres, C.V., & Blanco, M.N. (1996). Adsorption and impregnation of alumina with molybdenum or tungsten solutions. *Adsorption Science and Technology* 13 (3), 165-176.

Plyuto, Yu. V., Babich, I. V., Plyuto, I. V., Van Langeveld, A. D., & Moulijn, J. A. (1997). Synthesis and characterization of molybdenum(VI) oxo-species on the surface of fumed alumina and silica. *Colloids and Surfaces A: Physicochemical and Engineering Aspects*, 125 (2-3), 225-230.

Ramirez, J., Cedeno, L., & Busca, G. (1999). The Role of Titania Support in Mo-Based Hydrodesulfurization Catalysts. *Journal of Catalysis* 184 (1), 59-67.

Regalbuto, J. R., Navada, A., Shadid, S., Bricker, M. L., & Chen, Q. (1999). An Experimental Verification of the Physical Nature of Pt Adsorption onto Alumina. *Journal of Catalysis* 184 (2), 335-348.

Roukoss, C., Laurenti, D., Devers, E., Marchand, K., Massin, L., & Vrinat, M. (2009). Hydrodesulfurization catalysts: Promoters, promoting methods and support effect on catalytic activitie. *Comptes Rendus Chimie* 12 (6-7), 683-691.

Ruckenstein, E., & Karpe, P. (1989). Control of metal distribution in supported catalysts by pH, ionic strength, and coimpregnation. *Langmuir* 5 (6), 1393-1407.

Schmal, M., Baldanza, M. A. S., & Vannice, M. A. (1999). Pd-xMo/Al_2O_3 Catalysts for NO Reduction by CO. Journal of Catalysis 185 (1), 138-151.

Semagina, N., Kiwi-Minsker, L. (2009). Recent Advances in the Liquid-Phase Synthesis of Metal Nanostructures with Controlled Shape and Size for Catalysis. *Catalysis Reviews- Science and Engineering* 51 (2), 147 217.

Siri, G.J., Morales, M.I., Blanco, M.N., & Thomas, H.J. (1985). The $MoCoAl_2O_3$ system. I. Molybdenum adsorption on $CoAl_2O_3$. *Applied Catalysis* 19 (1), 49-63.

Spanos, N., & Lycourghiotis, A. (1994). Mechanism of codeposition of Mo(VI) species and Co^{2+} ions on the γ-alumina surface. *Langmuir* 10 (7), 2351-2362.

Spanos, N., Vordonis, L., Kordulis, Ch., & Lycourghiotis, A. (1990). Molybdenum-oxo species deposited on alumina by adsorption : I. Mechanism of the Adsorption. *Journal of Catalysis* 124 (2), 301-314.

Tamura, H., Katayama, N., & Furuichi, R. (1997). The Co^{2+} Adsorption Properties of Al_2O_3, Fe_2O_3, Fe_3O_4, TiO_2, and MnO_2 Evaluated by Modeling with the Frumkin Isotherm. *Journal of Colloid and Interface Science* 195 (1), 192-202.

Tewari, P.H., Campell A.B., & Lee, W. (1975). Adsorption of Co2+ by Oxides from Aqueous Solution. *Canadian Journal of Chemistry* 50 (11), 16421648.

van Veen, J.A.R., Hendriks, P.A.J.M., Romers, E.J.G.M., & Andrea, R.R. (1990). Chemistry of phosphomolybdate adsorption on alumina surfaces. 1. The molybdate/alumina system. *Journal of Physical Chemistry* 94 (13), 5275-5282.

Tomii, V., & Simeon, V. (1999). Ion association in aqueous solutions of strong electrolytes: a UVVis spectrometric and factor-analytical study. *Physical Chemistry Chemical Physics* 1 (2), 299-302.

van Veen, J. A. R., de Wit, H., Emeis, C. A., & Hendriks, P. A. J. M. (1987). On the adsorption of heptamolybdate ions on [gamma]-Al_2O_3 and TiO_2. *Journal of Catalysis* 107 (2), 579-582.

Vissenberg, M.J., Joosten, L.J.M., Heffels, M.M.E.H., van Welsenes, A.J., de Beer, V.H.J., van Santen, R.A., & van Veen, J.A.R. (2000). Tungstate versus Molybdate Adsorption on Oxidic Surfaces: A Chemical Approach. *Journal of Physical Chemistry* B 104 (35), 84568461.

Wang, L., & Keith Hall, W. (1982). The preparation and genesis of molybdena-alumina and related catalyst systems. *Journal of Catalysis* 77 (1), 232-241.

Weber R. S. (1995). Effect of Local Structure on the UV-Visible Absorption Edges of Molybdenum Oxide Clusters and Supported Molybdenum Oxides. *Journal of Catalysis* 151 (2), 470-474.

Weigold, H. (1983). The nature of molybdenum oxide species mounted on alumina: An oligomer model. *Journal of Catalysis*, 83 (1), 85-98.

Xiong, G., Feng, Z., Li, J., Yang, Q., Ying, P., Xin Q., & Li, C. (2000). UV Resonance Raman Spectroscopic Studies on the Genesis of Highly Dispersed Surface Molybdate Species on γ-Alumina. *Journal of Physical Chemistry*. B 104 (15), 35813588.